Ultrafast electrooptic dual-comb interferometry

Vicente Durán,[1] Santiago Tainta,[2] and Victor Torres-Company[1*]

[1]*Department of Microtechnology and Nanoscience, Chalmers University of Technology, SE 41296 Gothenburg, Sweden*

[2]*Department of Electrical and Electronic Engineering, Universidad Pública de Navarra, 31006 Pamplona, Spain*

[*]*torresv@chalmers.se*

Abstract: Dual-comb interferometry is a particularly compelling technique that relies on the phase coherence of two laser frequency combs for measuring broadband complex spectra. This method is rapidly advancing the field of optical spectroscopy and empowering new applications, from nonlinear microscopy to laser ranging. Up to now, most dual-comb interferometers were based on modelocked lasers, whose repetition rates have restricted the measurement speed to ~kHz. Here we demonstrate a dual-comb interferometer that is based on electrooptic frequency combs and measures consecutive complex spectra at an ultra-high refresh rate of 25 MHz. These results pave the way for novel scientific and metrology applications of frequency comb generators beyond the realm of molecular spectroscopy, where the measurement of ultrabroadband waveforms is of paramount relevance.

©2015 Optical Society of America

OCIS codes: (320.7100) Ultrafast measurements; (300.6310) Spectroscopy, heterodyne; (060.0060) Fiber optics and optical communications.

References and links

1. S. Schiller, "Spectrometry with frequency combs," Opt. Lett. **27**(9), 766–768 (2002).
2. F. Keilmann, C. Gohle, and R. Holzwarth, "Time-domain mid-infrared frequency-comb spectrometer," Opt. Lett. **29**(13), 1542–1544 (2004).
3. I. Coddington, W. C. Swann, and N. R. Newbury, "Coherent multiheterodyne spectroscopy using stabilized optical frequency combs," Phys. Rev. Lett. **100**(1), 013902 (2008).
4. B. Bernhardt, A. Ozawa, P. Jacquet, M. Jacquey, Y. Kobayashi, T. Udem, R. Holzwarth, G. Guelachvili, T. W. Hänsch, and N. Picqué, "Cavity-enhanced dual-comb spectroscopy," Nat. Photonics **4**(1), 55–57 (2010).
5. A. Klee, J. Davila-Rodriguez, C. Williams, and P. J. Delfyett, "Characterization of semiconductor-based optical frequency comb sources using generalized multiheterodyne detection," IEEE J. Sel. Top. Quantum Electron. **19**(4), 1100711 (2013).
6. A. M. Zolot, F. R. Giorgetta, E. Baumann, J. W. Nicholson, W. C. Swann, I. Coddington, and N. R. Newbury, "Direct-comb molecular spectroscopy with accurate, resolved comb teeth over 43 THz," Opt. Lett. **37**(4), 638–640 (2012).
7. A. Schliesser, M. Brehm, F. Keilmann, and D. van der Weide, "Frequency-comb infrared spectrometer for rapid, remote chemical sensing," Opt. Express **13**(22), 9029–9038 (2005).
8. F. Zhu, T. Mohamed, J. Strohaber, A. A. Kolomenskii, T. Udem, and H. A. Schuessler, "Real-time dual frequency comb spectroscopy in the near infrared," Appl. Phys. Lett. **102**(12), 121116 (2013).
9. S. Potvin and J. Genest, "Dual-comb spectroscopy using frequency-doubled combs around 775 nm," Opt. Express **21**(25), 30707–30715 (2013).
10. Z. Zhang, T. Gardiner, and D. T. Reid, "Mid-infrared dual-comb spectroscopy with an optical parametric oscillator," Opt. Lett. **38**(16), 3148–3150 (2013).
11. G. Villares, A. Hugi, S. Blaser, and J. Faist, "Dual-comb spectroscopy based on quantum-cascade-laser frequency combs," Nat. Commun. **5**, 5192 (2014).
12. G. B. Rieker, F. R. Giorgetta, W. C. Swann, J. Kofler, A. M. Zolot, L. C. Sinclair, E. Baumann, C. Cromer, G. Petron, C. Sweeny, P. P. Tans, I. Coddington, and N. R. Newbury, "Frequency-comb-based remote sensing of greenhouse gases over kilometer air paths," Optica **1**(5), 290–298 (2014).
13. T. Ideguchi, S. Holzner, B. Bernhardt, G. Guelachvili, N. Picqué, and T. W. Hänsch, "Coherent Raman spectro-imaging with laser frequency combs," Nature **502**(7471), 355–358 (2013).
14. I. Coddington, W. C. Swann, L. Nenadovic, and N. R. Newbury, "Rapid and precise absolute distance measurements at long range," Nat. Photonics **3**(6), 351–356 (2009).

#251112 Received 30 Sep 2015; revised 3 Nov 2015; accepted 3 Nov 2015; published 13 Nov 2015
© 2015 OSA

One print or electronic copy may be made for personal use only. Systematic reproduction and distribution, duplication of any material in this paper for a fee or for commercial purposes, or modifications of the content of this paper are prohibited.

15. S. Boudreau, S. Levasseur, C. Perilla, S. Roy, and J. Genest, "Chemical detection with hyperspectral lidar using dual frequency combs," Opt. Express **21**(6), 7411–7418 (2013).
16. T.-A. Liu, N. R. Newbury, and I. Coddington, "Sub-micron absolute distance measurements in sub-millisecond times with dual free-running femtosecond Er fiber-lasers," Opt. Express **19**(19), 18501–18509 (2011).
17. S. Boudreau and J. Genest, "Range-resolved vibrometry using a frequency comb in the OSCAT configuration," Opt. Express **22**(7), 8101–8113 (2014).
18. F. Ferdous, D. E. Leaird, C.-B. Huang, and A. M. Weiner, "Dual-comb electric-field cross-correlation technique for optical arbitrary waveform characterization," Opt. Lett. **34**(24), 3875–3877 (2009).
19. I. Coddington, W. Swann, and N. Newbury, "Coherent dual-comb spectroscopy at high signal-to-noise ratio," Phys. Rev. A **82**(4), 043817 (2010).
20. J. Roy, J.-D. Deschênes, S. Potvin, and J. Genest, "Continuous real-time correction and averaging for frequency comb interferometry," Opt. Express **20**(20), 21932–21939 (2012).
21. T. Ideguchi, A. Poisson, G. Guelachvili, N. Picqué, and T. W. Hänsch, "Adaptive real-time dual-comb spectroscopy," Nat. Commun. **5**, 3375 (2014).
22. T. Kobayashi, H. Yao, K. Amano, Y. Fukushima, A. Morimoto, and T. Sueta, "Optical pulse compression using high-frequency electro-optic phase modulation," IEEE J. Quantum Electron. **24**(2), 382–387 (1988).
23. T. Yamamoto, T. Komukai, K. Takada, and A. Suzuki, "Spectrally flattened phase-locked multi-carrier light generator with phase modulators and chirped fibre Bragg grating," Electron. Lett. **43**(19), 1040–1042 (2007).
24. T. Otsuji, M. Yaita, T. Nagatsuma, and E. Sano, "10-80 Gb/s highly extinctive electro-optic pulse pattern generator," IEEE J. Sel. Top. Quantum Electron. **2**(3), 643–649 (1996).
25. A. J. Metcalf, V. Torres-company, D. E. Leaird, S. Member, and A. M. Weiner, "High-power broadly tunable electrooptic frequency comb generator," IEEE J. Sel. Top. Quantum Electron. **19**(6), 350036 (2013).
26. V. Torres-Company and A. M. Weiner, "Optical frequency comb technology for ultra-broadband radio-frequency photonics," Laser Photonics Rev. **8**(3), 368–393 (2014).
27. S.-J. Lee, B. Widiyatmoko, M. Kourogi, and M. Ohtsu, "Ultra-high scanning speed optical coherence tomography using optical frequency comb generators," Jpn. J. Appl. Phys. **40**(Part 2, No. 8B), L878–L880 (2001).
28. T. Ohara, H. Takara, T. Yamamoto, H. Masuda, T. Morioka, M. Abe, and H. Takahashi, "Over-1000-channel ultradense WDM transmission with supercontinuum multicarrier source," J. Lightwave Technol. **24**(6), 2311–2317 (2006).
29. E. Hamidi, D. E. Leaird, and A. M. Weiner, "Tunable programmable microwave photonic filters based on an optical frequency comb," IEEE Trans. Microw. Theory Tech. **58**(11), 3269–3278 (2010).
30. A. Ishizawa, T. Nishikawa, A. Mizutori, H. Takara, H. Nakano, T. Sogawa, A. Takada, and M. Koga, "Generation of 120-fs laser pulses at 1-GHz repetition rate derived from continuous wave laser diode," Opt. Express **19**(23), 22402–22409 (2011).
31. R. Wu, V. Torres-Company, D. E. Leaird, and A. M. Weiner, "Supercontinuum-based 10-GHz flat-topped optical frequency comb generation," Opt. Express **21**(5), 6045–6052 (2013).
32. K. Beha, D. C. Cole, F. N. Baynes, P. Del'Haye, A. Rolland, T. M. Fortier, F. Quinlan, S. A. Diddams, and S. B. Papp, "Towards self-referencing a 10-GHz electro-optic comb," ED-1a.3 Mon Proc. CLEO Europe (2015).
33. D. A. Long, A. J. Fleisher, K. O. Douglass, S. E. Maxwell, K. Bielska, J. T. Hodges, and D. F. Plusquellic, "Multiheterodyne spectroscopy with optical frequency combs generated from a continuous-wave laser," Opt. Lett. **39**(9), 2688–2690 (2014).
34. P. Martin-Mateos, M. Ruiz-Llata, J. Posada-Roman, and P. Acedo, "Dual-comb architecture for fast spectroscopic measurements and spectral characterization," IEEE Photonics Technol. Lett. **27**(12), 1309–1312 (2015).
35. P. Martín-Mateos, B. Jerez, and P. Acedo, "Dual electro-optic optical frequency combs for multiheterodyne molecular dispersion spectroscopy," Opt. Express **23**(16), 21149–21158 (2015).
36. G. Millot, S. Pitois, M. Yan, T. Hovannysyan, A. Bendahmane, T. W. Hänsch, and N. Picqué, "Frequency-agile dual-comb spectroscopy," Arxiv 1505.07213 (2015).
37. T. Nishikawa, A. Ishizawa, M. Yan, H. Gotoh, T. Hänsch, and N. Picqué, "Broadband Dual-comb Spectroscopy with Cascaded-electro-optic-modulator-based Frequency Combs," in CLEO: 2015, OSA Technical Digest (online) (Optical Society of America, 2015), paper SW3G.2.
38. A. Ishizawa, T. Nishikawa, M. Yan, G. Millot, H. Gotoh, T. Hänsch, and N. Picqué, "Optical Frequency Combs of Multi-GHz Line-spacing for Real-time Multi-heterodyne Spectroscopy," in CLEO: 2015, OSA Technical Digest (online) (Optical Society of America, 2015), paper SW1G.7.
39. N. R. Newbury, I. Coddington, and W. Swann, "Sensitivity of coherent dual-comb spectroscopy," Opt. Express **18**(8), 7929–7945 (2010).
40. I. Coddington, W. C. Swann, and N. R. Newbury, "Coherent linear optical sampling at 15 bits of resolution," Opt. Lett. **34**(14), 2153–2155 (2009).
41. Z. Jiang, C.-B. Huang, D. E. Leaird, and A. M. Weiner, "Optical arbitrary waveform processing of more than 100 spectral comb lines," Nat. Photonics **1**(8), 463–467 (2007).
42. V. R. Supradeepa, D. E. Leaird, and A. M. Weiner, "Single shot amplitude and phase characterization of optical arbitrary waveforms," Opt. Express **17**(16), 14434–14443 (2009).
43. N. K. Fontaine, R. P. Scott, J. P. Heritage, and S. J. B. Yoo, "Near quantum-limited, single-shot coherent arbitrary optical waveform measurements," Opt. Express **17**(15), 12332–12344 (2009).

#251112 Received 30 Sep 2015; revised 3 Nov 2015; accepted 3 Nov 2015; published 13 Nov 2015
© 2015 OSA

44. V. R. Supradeepa, C. M. Long, D. E. Leaird, and A. M. Weiner, "Self-referenced characterization of optical frequency combs and arbitrary waveforms using a simple, linear, zero-delay implementation of spectral shearing interferometry," Opt. Express **18**(17), 18171–18179 (2010).
45. N. K. Fontaine, R. P. Scott, L. Zhou, F. M. Soares, J. P. Heritage, and S. J. B. Yoo, "Real-time full-field arbitrary optical waveform measurement," Nat. Photonics **4**(4), 248–254 (2010).
46. S. Yamashita and T. Okoshi, "Suppression of Beat Noise from Optical Amplifiers Using Coherent Receivers," J. Lightwave Technol. **12**(6), 1029–1035 (1994).
47. A. Ishizawa, T. Nishikawa, A. Mizutori, H. Takara, S. Aozasa, A. Mori, H. Nakano, A. Takada, and M. Koga, "Octave-spanning frequency comb generated by 250 fs pulse train emitted from 25 GHz externally phase-modulated laser diode for carrier-envelope-offset locking," Electron. Lett. **46**(19), 1343–1344 (2010).
48. V. Ataie, E. Myslivets, B. P.-P. Kuo, N. Alic, and S. Radic, "Spectrally equalized frequency comb generation in multistage parametric mixer with nonlinear pulse shaping," J. Lightwave Technol. **32**(4), 840–846 (2014).
49. T. J. Kippenberg, R. Holzwarth, and S. A. Diddams, "Microresonator-based optical frequency combs," Science **332**(6029), 555–559 (2011).
50. C. Y. Wang, T. Herr, P. Del'Haye, A. Schliesser, J. Hofer, R. Holzwarth, T. W. Hänsch, N. Picqué, and T. J. Kippenberg, "Mid-infrared optical frequency combs at 2.5 μm based on crystalline microresonators," Nat. Commun. **4**, 1345 (2013).
51. X. Xue, Y. Xuan, P. H. Wang, Y. Liu, D. E. Leaird, M. Qi, and A. M. Weiner, "Normal-dispersion microcombs enabled by controllable mode interactions," Laser Photonics Rev. **9**(4), 23–28 (2015).
52. S. A. Miller, Y. Okawachi, S. Ramelow, K. Luke, A. Dutt, A. Farsi, A. L. Gaeta, and M. Lipson, "Tunable frequency combs based on dual microring resonators," Opt. Express **23**(16), 21527–21540 (2015).
53. D. R. Solli, J. Chou, and B. Jalali, "Amplified wavelength-time transformation for real-time spectroscopy," Nat. Photonics **2**(1), 48–51 (2008).

1. Introduction

The dual-comb spectrometer (also known as dual-comb interferometer) is an instrument that unlocks the full potential of laser frequency combs for high-precision spectroscopy [1–6]. The features of a dual-comb spectrometer are simply unattainable with state-of-the-art Fourier transform spectrometers. For example, it offers a spectral resolution capable to resolve the individual frequency components of the comb. It can also scan terahertz bandwidth spectra at high signal-to-noise ratio (SNR) in relatively fast acquisition times (from milliseconds to a few seconds) because it is free from mechanical moving parts [3]. This technique has been successfully applied at different wavelength regions [7–11] and in modern spectroscopy applications, such as remote sensing of greenhouse gases [12] and nonlinear hyperspectral microscopy [13]. An additional characteristic of a dual-comb spectrometer is that it can retrieve the spectral phase of the sample under test. This has triggered applications different than molecular spectroscopy, such as coherent LIDAR [14–16], vibrometry [17] or the analysis of optical telecommunication components [18].

Most dual-comb interferometers presented to date make use of fiber or Ti:Sa modelocked laser technology. The repetition rate frequency of these laser sources typically lies in the 10-100 MHz range. This comb spacing provides a spectral resolution more than adequate for molecular spectroscopy, but introduces a fundamental limit in the speed that it takes to capture the optical spectrum (typically in the millisecond range). Longer acquisition times are often necessary in order to improve the SNR of the measurement by coherently averaging successive spectra [19]. Long acquisition times introduce stringent demands on the phase locking of the two combs employed in the dual-comb spectrometer, whose relative phase drifts need to be compensated for. This issue can be solved by using combs locked to external optical references (and therefore providing long-term stability [3]) or in free-running modelocked lasers by either applying real-time signal processing techniques [20] or adapting dynamically the sampling clock rate of the dual-comb spectrometer to the relative drift of the combs' offset and spacing [21]. Outstanding SNRs corresponding to > 20 bits have been reported for measurements accumulated in the course of 24 hrs using real-time signal processing [20].

The electrooptic modulation method is an alternative technique for producing coherent frequency combs (see e.g [24–26].). In essence this technique introduces optical sidebands around a continuous-wave laser by electrooptic modulation. The central frequency is given by

#251112 Received 30 Sep 2015; revised 3 Nov 2015; accepted 3 Nov 2015; published 13 Nov 2015
© 2015 OSA

the laser frequency and the external radio-frequency oscillator provides the line spacing of the comb. There are two basic configurations to implement this technique. The first one, based on the placement of a phase modulator inside a Fabry-Perot cavity, attracted significant attention before the introduction of self-referenced mode-locked lasers (for a review see [26]). In fact, this type of electrooptic frequency combs was used in the first reported dual-comb interferometer, conceived to perform optical coherence tomography [27]. However, this cavity-based approach requires an active and precise stabilization scheme to lock the input laser frequency to a cavity resonance. The second approach to electrooptic generation consists of using a chain of electrooptic modulators. This scheme allows tuning in an independent and continuous manner the offset and line spacing of the comb [25]. In addition, it is assembled with standard optical telecommunication equipment and indeed has been used as a source for lightwave communications [28] and radio-frequency photonics [26, 29]. Electrooptic comb generators have gained momentum in the last years thanks to advances in fiber laser technology, high-performance lithium niobate modulators and microwave dielectric resonator oscillators [26]. The optical spectrum of an electrooptic comb can be substantially broadened in a highly nonlinear fiber [30, 31] and there is recent progress towards achieving self-referencing [32], an important ingredient for absolute metrology. Very recently, several groups have implemented dual-comb spectroscopy with frequency combs formed by phase and/or intensity electrooptic modulators [33–38]. The rationale lies in the robustness and simplicity in the hardware implementation of such electrooptic dual-comb spectrometers. In addition, the fact that a single laser feeds the two combs ensures the necessary phase locking by default [33] without the need for complex feedback stabilization mechanisms.

Here we uncover an additional benefit of an electrooptic dual-comb spectrometer, namely the possibility to operate at ultra-high speeds of tens of MHz. This is due to the fact that an electrooptic comb generator operates at repetition rates in the 10 GHz range and therefore has a few lines covering a broad bandwidth. We show that this trade in spectral resolution can be used to increase the measurement speed while affecting neither the measurement bandwidth nor the accuracy. We report complex spectral measurements spanning over a terahertz bandwidth in the telecommunications C band. Standard radio-frequency equipment is employed to perform arbitrary optical waveform characterization at acquisition times of tens of ns. The phase performance achieved in a single interferogram is significant (~30 mrad accuracy). This is due to the fact that electrooptic combs concentrate the available power in tens of lines (as opposed to tens of thousands in fiber modelocked lasers), hence achieving higher signal to noise ratio per spectral bin. We show that coherent averaging can be performed over thousands of interferograms to either increase the system sensitivity or to recover signals at an ultra-low power level. Either configuration still preserves an effective measurement time at the sub-millisecond scale. These results pave the way to utilize the dual-comb technique in scientific applications different than spectroscopy, especially for those that require robust and accurate measurements of broadband waveforms at ultra-high speeds.

2. Dual-comb interferometry

2.1 Operation principle

The operation principle of dual-comb spectroscopy can be understood in two equivalent ways [6]. In the time domain, the complex amplitude of a sample is encoded on the spectrum of a train of pulses with repetition rate f_s. This optical signal interferes with a reference train of pulses that has a slightly different repetition rate $f_r = f_s \pm \delta f$. The frequency offset, δf, makes the pulses from each comb to overlap on the detector at varying time delays. As a result, the interference signal becomes the electric-field cross-correlation between the sample and the reference combs. A Fourier transform analysis of every interferogram provides the complex amplitude of the sample assuming the reference is known. Therefore, a dual-comb

#251112 Received 30 Sep 2015; revised 3 Nov 2015; accepted 3 Nov 2015; published 13 Nov 2015
© 2015 OSA

spectrometer essentially works as a 'virtual' scanning interferometer or, alternatively, as linear coherent sampling.

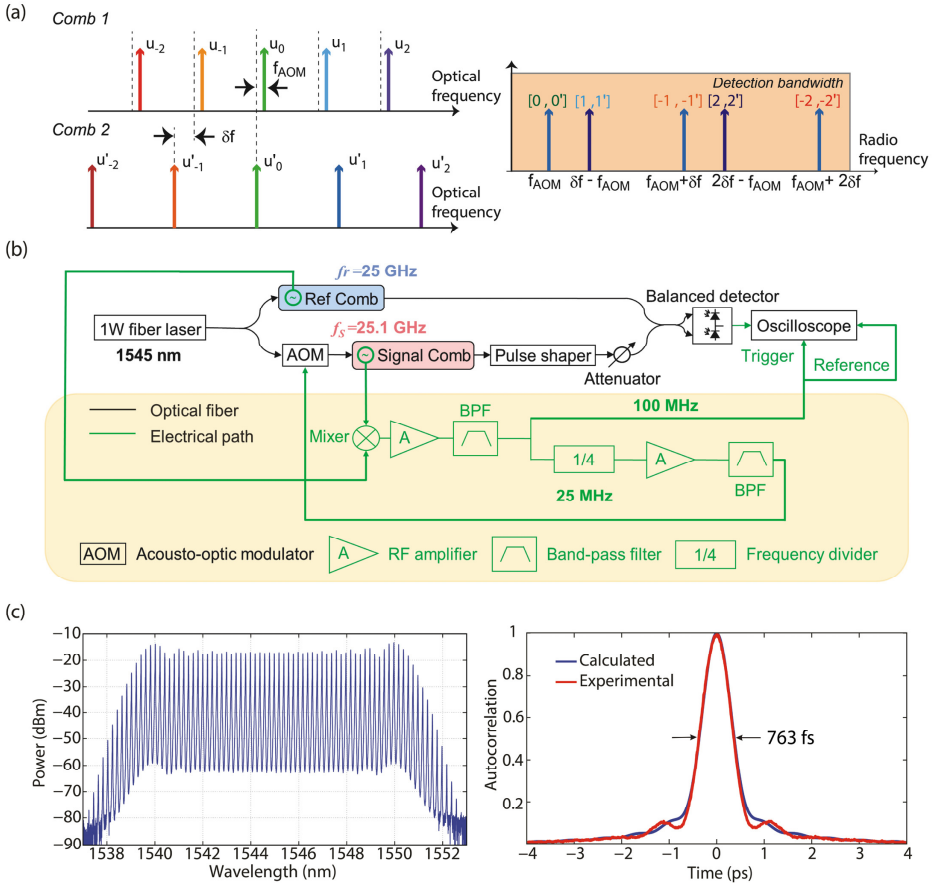

Fig. 1. (a) In the frequency domain, the multiheterodyne interference of two combs is interpreted as a downconversion of optical frequencies. The result is two interlaced combs in the radio-frequency domain. The radio frequencies are labeled by pairs of numbers that identify the beat between the mother optical comb lines u' and u'_i (i = –2,…,2). (b) Schematic of the experimental setup. Basically, it consists of a fiber heterodyne interferometer, being the signal and the local oscillator two electro-optic frequency combs fed by a high-power continuous-wave laser. The spectroscopy sample is an optical pulse shaper that allows us to synthesize the optical lines of the signal comb with a spectral resolution compatible with the repetition rate of the comb. (c) Optical spectrum at the output of the reference comb generator. Measured autocorrelation trace after compression (red line) and expected autocorrelation calculated assuming a flat spectral phase (blue line).

In the frequency-domain picture, the interference between the sample and reference leads to a multi-heterodyne detection process, since each line of the signal comb beats with the lines from the reference. The resulting beat notes are distributed in groups (Nyquist zones) along the radio-frequency region, leading to downconversion of the optical frequencies. Usually, one only considers the part of the radio-frequency spectrum that corresponds to the first Nyquist zone (which spans from dc to half the smaller of the two comb repetition rates). In an electrooptic dual-comb spectrometer, the same laser feeds the two combs, so that the spectra share the central frequency. As a result, pairs of lines in the upper and lower sidebands produce beat notes at exactly the same frequency. To avoid this ambiguity, we follow the scheme first proposed in [18] and shift the frequency of the laser with the aid of an acousto-

#251112 Received 30 Sep 2015; revised 3 Nov 2015; accepted 3 Nov 2015; published 13 Nov 2015
© 2015 OSA

optic modulator placed before one of the comb generators. Despite the hardware similarities between our approach and that work, there is an important conceptual difference between them. The frequency shift f_{AOM} introduced by the acousto-optic modulator in the mentioned reference is orders of magnitude greater than the comb frequency offset, $\delta f \ll f_{AOM}$. This configuration produces in the time domain an electric signal that is basically a fringe pattern (with a period of $1/f_{AOM}$) modulated by an envelope that resembles the amplitude of the cross-correlation between the sample and the reference fields. In the frequency domain, the resulting RF comb spectrum is localized in a small region around f_{AOM} and can be easily filtered. In our system, the acousto-optic frequency is an integer fraction of the frequency offset, so that both values are of the same order ($f_{AOM} \lesssim \delta f$) and commensurate, i.e. $f_{AOM} = \delta f / k$, being k an integer. This condition can be fulfilled with an appropriate RF circuit for driving the acousto-optic modulator, as is explained in the next section. The interference between the signal and the reference combs generates a temporal trace, which is modulated by a slowly varying envelope. This envelope determines the duration of an interferogram, which is composed of a series of rapidly oscillating waveforms. In the frequency-domain picture, the shift f_{AOM} moves the interference between the central comb lines away from dc and creates two interlaced radio-frequency combs in the downconversion process [11, 35]. Each radio-frequency comb has a frequency spacing δf, but a different offset that depends on f_{AOM}. Taking into account that the refresh rate will be given by the frequency location of the beat note closest to dc, a suitable selection of both f_{AOM} and δf can be chosen to optimize the measurement rate. This is particularly relevant for electrooptic combs, which have a few lines and therefore can be widely spread across the detection bandwidth.

2.2 Experimental setup

Our experimental setup is shown in Fig. 1(b). We set two electrooptic combs operating at ~25 GHz repetition rate with an offset of $\delta f = 100\,\mathrm{MHz}$ and $f_{AOM} = 25\,\mathrm{MHz}$. In this manner, it is the frequency offset between the central lines of the combs that determines the maximum refresh rate. Each comb generator is composed of an intensity modulator followed by a pair of phase modulators. These commercially available devices are based on lithium niobate electrooptic modulators and are specially designed to handle high power (both from the microwave source and the input laser). The modulators are driven by a commercial low-phase-noise dielectric resonator oscillator (−100 dBc/Hz at 1 kHz offset). The continuous-wave laser is a low RIN, low linewidth (~10 kHz), fiber laser centered at 1545 nm whose power is boosted to 1W by an erbium-doped amplifier. The low linewidth laser tolerates delay differences between the interferometer arms of up to ~100 microseconds and hence allows measuring spectroscopic signals with long interaction lengths. The intensity modulator is biased to provide a train of pseudo-square pulses with ~50% duty cycle. The chirp of the phase modulators is aligned to the square pulses with tunable microwave phase shifters. The intensity modulator blocks the light when the chirp from the phase modulators is mostly linear. In this way, the comb spectrum becomes relatively flat [24]. The use of two phase modulators in tandem enables to increase the effective modulation index and hence the comb bandwidth. Our arrangement provides 55 lines at −10 dB bandwidth (or 1.4 THz optical bandwidth), as can be observed in Fig. 1(c) for the reference comb. The loss of each comb generator is ~-15 dB. The layout of the combs is similar to the one in [25]. As in this work, we found the power spectrum of the comb to remain stable for several hours without the need for active feedback stabilization in the dc bias. Figure 1(c) also shows the measured autocorrelation trace (red line) after imparting onto the reference spectrum a pure quadratic

#251112 Received 30 Sep 2015; revised 3 Nov 2015; accepted 3 Nov 2015; published 13 Nov 2015
© 2015 OSA

phase, which leads to the pulse compression achievable with dispersive fiber alone. This trace is compared to that corresponding the transform-limited case (blue line), which was calculated assuming a flat spectral phase. Similar results are obtained for the signal comb.

The light emerging from the spectroscopic sample is controlled by a variable optical attenuator and combined with the reference comb on a 50:50 coupler. The interference is measured by a balanced detector (BD, from u2t Photonics AG, model BPDV2150R). The balanced detection avoids the 3-dB power penalty inherent to the mixing process and eliminates the unwanted dc term that comes with the interference signal. In both arms, polarization controllers are inserted at the entrance of each comb and just before the final coupler to optimize the measured optical power. The radio-frequency signal generated by the detector is digitized by an 8 bits oscilloscope with 3 GHz bandwidth (LeCroy Wavemaster 8300), which registers a temporal trace during a total record time of 200 μs at a sampling rate of 10 GS/s. The output of the photodetector is low-pass filtered and amplified by a stage of three low-noise microwave amplifiers to make an optimal use of the available bits in the detection unit.

An important aspect of the setup here presented is that it is self-synchronized and the sampling stage is commensurate to the frequency offsets. This alleviates the digital signal processing and any drift in the repetition rate of the comb is automatically taken into account at the sampling stage. The RF circuit included in our setup is shown in the yellow box in Fig. 1(b). The offset in repetition rate frequencies is extracted via a mixer. One half of the signal at the output of the mixer is used as both external clock and trigger for the oscilloscope. The other half passes through a frequency divider to produce a radio-frequency signal whose frequency is reduced by a factor 4. This signal, after being amplified and filtered, drives the acousto-optic modulator.

Our dual-comb spectrometer requires a calibration process to work. In a preliminary experiment, the spectroscopic sample in the signal arm is removed. The pulses emerging from the reference are compressed by means of dispersive fiber to near their transform-limited duration, so the cross-correlation peak between the LO and the sample combs is optimized. This measurement provides the default complex amplitude between interferometer arms. As a first test for our system, 99.84 m of single-mode fiber (SMF-28-100 from Thorlabs) is then inserted in the signal arm as the spectroscopic sample. From the interferogram measurements, we calculate the quadratic spectral phase introduced by the fiber test, providing a dispersion parameter of D = 17.25 ps /km nm, close to the value specified by the manufacturer (D≤18 ps /km nm). The mean phase error of our measurement is ~49 mrad, similar to the values achieved for the different spectroscopic examples provided in Section 3. This independent verification indicates that it is the dual electrooptic comb system (concretely the signal to noise ratio of the comb lines) what provides the limit in phase performance.

In subsequent experiments, the spectroscopic sample is emulated by a commercial pulse shaper (Finisar 4000 S) with 10 GHz resolution and 1 GHz accuracy, which is used to synthesize the spectrum of the signal comb in a line-by-line manner. After inserting the pulse shaper in the signal arm, the above calibration process is repeated. Concretely, the pulse shaper is initially configured to compress the pulses in the signal arm before adding the spectral function under study. Although this preliminary step is not strictly necessary, it helps in achieving a flat spectral phase in the calibration phase profile (apart from a linear term).

2.3 Signal-to-noise ratio

For each comb line, the error on the phase $\epsilon_\varphi(\nu)$ can be calculated as the standard deviation of the set of values obtained from the sequence of Fourier-transformed interferograms. Assuming that the retrieved power spectrum $S(\nu)$ has the same error in each quadrature, the inverse of the phase error, $\epsilon_\varphi^{-1}(\nu)$, gives the frequency-domain signal-to-noise ratio SNR_f,

#251112 Received 30 Sep 2015; revised 3 Nov 2015; accepted 3 Nov 2015; published 13 Nov 2015
© 2015 OSA

defined as $SNR_f(\nu) = |S(\nu)| / \sigma_\nu$, where σ_ν is the standard deviation of the amplitude $|S(\nu)|$ of the spectrum [39]. For our set of 2500 interferograms, the phase error averaged over all comb lines when the pulse shaper is programmed to compress the signal pulses is ϵ_φ = 57 mrad. From ϵ_φ, the signal-to-noise ratio results $SNR_f = 17.7$. A similar value is obtained by calculating SNR_f from its definition ($SNR_f = 17.5$). In order to measure the peak time-domain signal-to-noise ratio SNR_t, we calculate the temporal profile of the electric field in the signal arm. From the set of retrieved fields, SNR_t is calculated as the ratio between the maximum field amplitude and the corresponding mean error [40], giving $SNR_t = 119$. The above results were obtained when the average optical power before the detector was 1 mW in both interferometer arms. The value obtained for SNR_t is roughly four times lower than the one corresponding to the shot-noise limit, $\sqrt{2\eta n_s} = 472$, where η is the detector efficiency and n_s is the average number of photons per signal pulse [39]. Within a good approximation, this value is related to that obtained for SNR_f by a factor $\sqrt{M}$, being M the number of comb lines.

3. Optical arbitrary waveform characterization

The spectroscopy examples in this section correspond to synthetic waveforms programmed in the sample arm with the aid of a reconfigurable complex filter (a pulse shaper). In our case the shaper resolution is better than the comb spacing. This corresponds to the line-by-line regime and the synthesized waveforms may have a duty cycle approaching 100% [41]. We choose this coherent regime because it introduces great challenges for any measurement technique owing to the possible overlap at the period boundaries between consecutive pulses in the train [42–45].

Figure 2(a) shows an oscilloscope trace measured during 10 μs for a train of pulses with a cubic spectral phase. The periodicity of the registered electrical signal is made evident in the lower inset of Fig. 2(a). The function programmed onto the pulse shaper is the superposition of two terms. The first one is an approximately quadratic function that compensates for the phase of the comb and produces a train of transformed-limited pulses. The other term is the cubic phase imparted onto the spectrum, plotted in the left inset of Fig. 2(b). The duration of an interferogram is $T = 1/f_{AOM} = 40\,\text{ns}$, so a complete temporal trace recorded by the oscilloscope contains 5000 interferograms, each one formed by four consecutive 10-ns electrical waveforms. In order to sample the successive interferograms, we use as a reference clock the 100-MHz signal generated by the mixer shown in Fig. 1(b). For each interferogram, the spectral complex amplitude is recovered through an FFT routine, which includes conventional tools in FFT analysis, such as zero padding or phase unwrapping. Figure 2(b) shows the set of temporal intensity profiles for a 20-ps window calculated from 2500 interferograms (half of the recorded temporal trace). The signal coming from the pulse shaper is also recorded by a commercial optical sampling scope (green curve). The result provided by the dual-comb technique has significantly better stability and temporal resolution because of the tight phase locking between combs and the inherent broadband operation.

Next we explore the synthesis of optical waveforms with duty cycles of ~100%. To this end, we impart onto the sample comb spectrum a phase profile corresponding to a sinusoidal phase function with an abrupt phase change of π, shown in the blue curve in Fig. 3(a). As before, we analyze half of the recorded temporal trace, which contains 2500 interferograms. The retrieved spectral phase, measured from a single interferogram, is shown in Fig. 3(a) (green points). These phase values are therefore obtained at a refresh rate of 25 MHz. In the course of these measurements, we realized that the phase sensitivity of the dual-comb

#251112 Received 30 Sep 2015; revised 3 Nov 2015; accepted 3 Nov 2015; published 13 Nov 2015
© 2015 OSA

technique is better than the nominal phase setting accuracy of the pulse shaper (~0.1 rad). To estimate the precision of our measurements, we calculated the standard deviation of the 2500 retrieved phases for each comb line. The result can be observed in Fig. 3(b). The mean value of the phase error $\epsilon_\varphi(\nu)$ is 32 mrad, which is equivalent to an optical path difference of ~8 nm at 1545 nm (or ~λ/193). It should be noted that $\epsilon_\varphi(\nu)$ depends slightly on the particular phase profile imparted onto the sample spectrum, as can be observed by comparing it with that obtained for the calibration measurement.

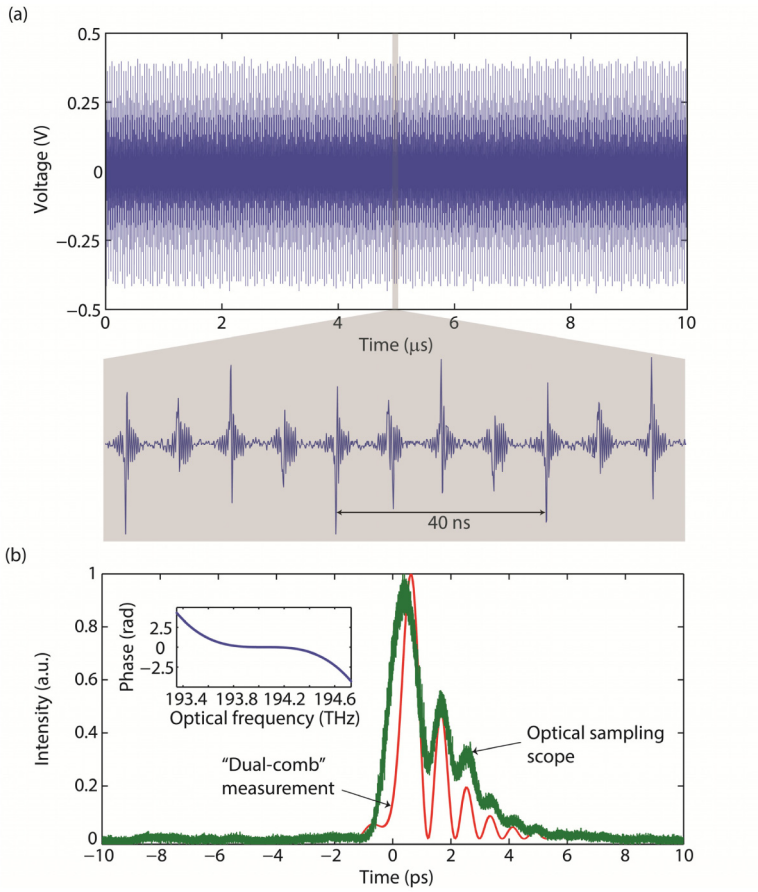

Fig. 2. Example of an arbitrary optical waveform characterization of a train of pulses with cubic phase. (a) Voltage measured by the oscilloscope during 10 μs (5% of the total record length). The periodicity of the recorded signal can be observed in the zoomed image included in the lower inset. (b) Intensity profile inside a 20-ps time window corresponding to the programmed spectral phase. The red profile is formed by the set of curves calculated from the recovered spectral phases corresponding to 2500 individual waveforms. The programmed phase profile is shown on the left. The green curve is the temporal signal recorded by a commercial optical sampling scope with limited temporal resolution (1 ps).

Figure 3(c) compares an autocorrelation measurement of the generated waveform (red line) with the autocorrelation function theoretically calculated from the spectral phase retrieved by means of the dual-comb technique (blue line). A commercial autocorrelator, placed at the end of the signal arm, measures a curve composed of 1000 points during 50 s. The theoretical line, in its turn, is calculated from the spectral phases obtained for a 100-μs temporal trace. The nonzero values of the autocorrelation function at the edges of the period demonstrate interference between neighbor pulses, i.e. a duty cycle close to 100%. The close

#251112 Received 30 Sep 2015; revised 3 Nov 2015; accepted 3 Nov 2015; published 13 Nov 2015
© 2015 OSA

match between the experimental and calculated curves corroborates the accuracy of our method when compared to a well-established pulse characterization technique. Figure 3(d) shows the superimposed intensity pulse profiles of 2500 waveforms calculated from the dual-comb technique. The fine line of this multivalued curve indicates very low intensity fluctuations (below 10^{-4} at the highest peak).

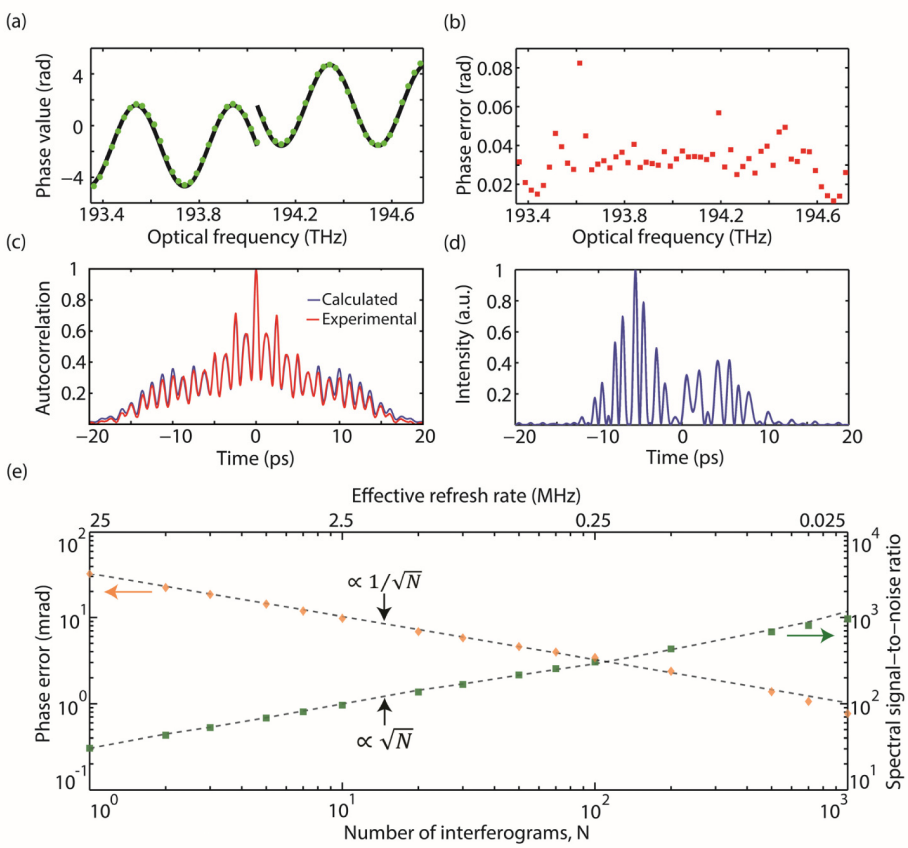

Fig. 3. Single-interferogram characterization of a 100% duty factor waveform. (a) Phase profile imparted onto the signal spectrum by the pulse shaper (blue curve) and spectral phases obtained from a single interferogram (arbitrarily chosen at half the temporal trace under analysis). (b) Standard deviation of the recovered phase for each comb line. (c) Autocorrelation function corresponding to the waveform generated by the line-by-line shaping. (d) 2500 overlaid intensity profiles built from the electrooptic dual-comb measurements. (e) Mean phase error and spectral signal-to-noise ratio when coherent averaging is performed. The points correspond to experimental data and the dashed lines are a theoretical fit.

One advantage of performing fast measurements is the possibility of using coherent averaging to increase the SNR (at the expense of reducing the measurement refresh rate). In particular, the SNR scales as $\sqrt{N}$ in either the frequency or the time domains, being N the number of averaged interferograms [39]. Therefore, the mean phase error for a single interferogram $\epsilon_\varphi^{N=1}$ is reduced by a factor $1/\sqrt{N}$ for an effective refresh rate of $(25/N)$ MHz. Figure 3(e) shows the evolution of ϵ_φ and SNR_f (calculated from its definition) when coherent averaging is performed for the above sinusoidal phase function with a π-jump. The dashed lines represent a fit assuming the theoretical dependence on $\sqrt{N}$. When N = 1000 interferograms are averaged (that is, for the minimum refresh rate considered here), the

#251112 Received 30 Sep 2015; revised 3 Nov 2015; accepted 3 Nov 2015; published 13 Nov 2015
© 2015 OSA

optical path difference is on the subnanometer scale (around 250 pm or λ/6200), which corresponds to a power signal-to-noise ratio per spectral component of 60 dB.

4. Sensitivity analysis in a preamplified configuration

The tradeoff between sensitivity and speed is an inherent feature of dual-comb spectroscopy. The ultrafast single-interferogram acquisition speeds achieved in our method permit to recover extremely weak signals (orders of magnitude lower than the local oscillator) and still operate at an effective refresh rate in the kHz regime. This improvement in sensitivity is especially desirable for illuminating targets at low power levels (an essential issue, for instance, to avoid damage in biological specimens) or when highly absorbing or scattering samples are considered.

To analyze the performance of our system, we systematically reduce the light power P_s coming from the pulse shaper with the aid of an attenuator, as indicated in Fig. 1(b). The spectral phase chosen for this experiment is a continuous sinusoidal function programmed in a line-by-line manner. The sensitivity can be enhanced by means of a pre-amplified detection scheme so that the signal's power level (measured before the optical amplifier) corresponds to pulses containing on average just a few photons. In particular, an erbium-doped fiber amplifier is inserted in the signal arm. We ensure that the average power arriving to the balanced detector remains constant (around 0 dBm). Depending on the degree of signal attenuation, an extra fiber amplifier can be included in cascade. This combination of pre-amplification and balanced detection is especially beneficial, since only the beating between the amplified spontaneous emission and the local oscillator gives a relevant noise term [46]. After the insertion of the fiber amplifier in the sample arm, we recalibrated the system following the process explained in Section 2.

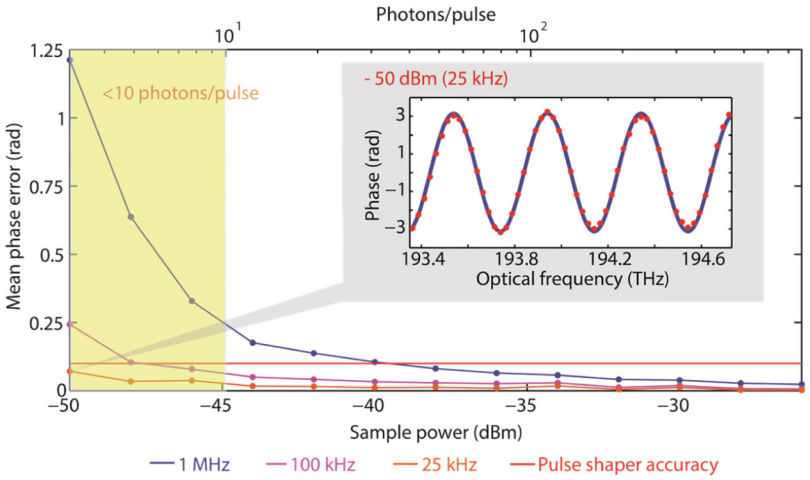

Fig. 4. Analysis of the system sensitivity in a pre-amplified detection scheme. The plot shows the mean phase error as a function of the signal power for three different effective refresh rates. The shadowed zone corresponds to signal pulses that on average have only a few photons. The recovered phase for P_s = –50 dBm (at 25 kHz effective refresh rate) is included in the inset. In this graph, the match of the phase values with the programmed curve is lower than the pulse shaper accuracy (0.1 rad) along the bandwidth of the comb.

Figure 4 shows the phase accuracy achieved by this configuration when the signal power is progressively decreased. At an effective refresh rate of 1 MHz, the mean phase error remains below 0.1 rad up to –39 dBm. However, for weaker signals, the amplified spontaneous emission noise in the preamplifier becomes predominant and the phase error increases. By averaging more spectral phases the SNR improves and therefore the error

#251112 Received 30 Sep 2015; revised 3 Nov 2015; accepted 3 Nov 2015; published 13 Nov 2015
© 2015 OSA

decreases. At an effective refresh rate of 100 kHz, the mean phase error exceeds the pulse shaper accuracy for $P_s \lesssim -48$ dBm. By reducing the effective refresh rate to 25 kHz (i.e. four times more waveforms averaged), it is still possible to recover the programmed phase function at −50 dBm, that is, a pulse waveform containing 3 photons on average. The recovered spectral phase for this minimum signal power is shown in the inset in Fig. 4. The difference between the experimental phase values and those programmed onto the pulse shaper is comparable to that observed, for example, in Fig. 3(a) for 0 dBm at 25 MHz. For effective refresh rates below a few MHz, a preprocessing of the measured data becomes possible. In that case, we calculate the FFT of the complete temporal trace and remove undesired spurious RF frequencies. The filtering process is accomplished by means of a bandpass comb filter, which is composed of teeth that are centered on the frequencies of interest. The bandpass is the same for every teeth and its bandwidth fixes the number of waveforms that can be averaged.

5. Discussion

Any dual-comb spectrometer shows a fundamental tradeoff among the number of lines, optical bandwidth, refresh rate and detector's dynamic range. Hitherto most dual-comb configurations have been based on femtosecond modelocked combs, which provide a spectral resolution (line spacing) in the MHz regime and cover several terahertz of spectral bandwidth. This choice allows for using low bandwidth detectors (~100 MHz) with high dynamic range (~16 bits), but it comes at the expense of a limit in the refresh rate (roughly a millisecond for a single interferogram).

In the electrooptic dual-comb technique, terahertz bandwidth spectra modulate a lower number of comb lines (~50-100), which can be used to boost the refresh rate by several orders of magnitude as shown in this work. Here the trade is in the spectral resolution (~10 GHz) and a lower dynamic range in the detection scheme (~8-10 bits for a few GHz of bandwidth). However, the electrooptic comb technique provides a great flexibility in reconfiguring the repetition rate and synchronizing to external sources [26]. Indeed, it is possible to realize external gating (hence decrease the repetition rate of the comb) and broaden the optical bandwidth by the use of highly non-linear optical fibers [47]. This has been recently exploited in [36] to realize an electrooptic dual-comb interferometer with a performance in terms of spectral resolution (and refresh rate) comparable to what can be achieved with fiber modelocked lasers.

It is interesting to look at the prospects and challenges in implementing dual-comb spectroscopy with ultra-high repetition-rate combs, such as those provided by parametric [48] or microresonator frequency combs [49]. In this case, ultra-high single-interferogram refresh rates (≥100 MHz) could be achieved (assuming optimally spread RF beat notes within the first Nyquist zone, as depicted in Fig. 1). However, a detection unit with broader bandwidth (tens of GHz) is required, which limits the dynamic range to 3-4 bits mainly due to sampling electronic jitter. Microresonator combs offer the prospect of realizing photonic integration [49] as well as exploring new wavelength windows [50]. In addition, there is recent progress in realizing coherent broadband microresonator combs with tunable line spacing and frequency offset [51,52]. These are indeed key ingredients to realize dual-comb spectroscopy with this platform.

The fastest technique that measures optical waveforms in a line-by-line manner is full-field coherent arbitrary waveform measurement [44]. This technique is highly suitable for coherent communication applications where the signal waveform needs to be measured at the baud rate. The hardware implementation is challenging though, since it requires N tightly synchronized coherent receivers with a bandwidth equal to the comb rate for N comb lines. In contrast, the dual-comb technique is multi-heterodyne and therefore a single, relatively low-

#251112 Received 30 Sep 2015; revised 3 Nov 2015; accepted 3 Nov 2015; published 13 Nov 2015
© 2015 OSA

frequency-bandwidth acquisition unit (3 GHz in this work) is required to measure a broadband waveform composed of tens of lines.

Finally, to put things in context, the resulting spectral resolution, bandwidth and refresh rate here reported are comparable to the performance achieved by the dispersive Fourier transformation technique [53]. A key distinctive aspect in dual-comb spectroscopy is that by default the setup is sensitive to the spectral phase of the sample and does not require a dispersive medium with distributed amplification to operate above the thermal-noise regime. In addition, with lithium niobate modulators, the wavelength operation range can be designed anywhere within ~0.8-2 μm. The scaling of the refresh rate in the dual-comb technique is highly favorable and for combs with multi-terahertz optical bandwidth at ~25 GHz repetition rates, it should be possible to maintain the ultrafast refresh rate utilizing a state-of-the-art sampling unit with tens of GHz analog bandwidth.

6. Conclusions

We have demonstrated that the electrooptic dual-comb technique allows measuring broadband optical waveforms at ultra-high single-interferogram refresh rates (up to 25 MHz). To this end, we have presented a self-synchronized interferometer composed of two electroooptic frequency combs. This system has been configured so that the high repetition rate of such combs (25 GHz) is exploited to maximize the measurement refresh rate. To check the system performance, spectral phases corresponding to 100% duty cycle waveforms have been recovered with a mean phase error of tens of mrad in a single interferogram (below the accuracy of the commercial pulse shaper employed as the spectroscopy sample). Finally, coherent averaging has been used to either improve the phase resolution below the mrad level or recover ultra-low-power signals (3 photons/pulse on average) while preserving measurement speed around tens of microseconds.

Regarding applications, the ability to measure arbitrary terahertz bandwidth waveforms in the sub-microsecond regime opens up new prospects in ultrafast metrology. We mention, for example, frequency domain reflectometry and optical coherence tomography; the measurement of telecommunication equipment in absence of slow environmental drifts affecting the measurement; dynamic profilometry of surfaces in industrial machining; and high-speed phase-sensitive imaging.

Acknowledgments

The authors are thankful to Peter Andrekson and Andrew Weiner for technical discussions and support.

This work has been funded by the Swedish Research Council (VR, grant number 048701). VD acknowledges funding from a Marie Curie Intra European Fellowship (PIEF-GA-2013-625121) and VTC a Marie Curie Career Integration grant (PCIG13-GA-2013-618285). ST acknowledges funding from the Spanish Ministry of Science and Innovation (project TEC2010-21303-04-01).

#251112 Received 30 Sep 2015; revised 3 Nov 2015; accepted 3 Nov 2015; published 13 Nov 2015
© 2015 OSA

130.206.158.161 {ts '2020-08-25 05:26:37'}